

# COMPENSATION GROUTING IN PERTH CBD AND ITS NUMERICAL BACKANALYSIS

Gima V. Mathew and Barry M. Lehane

*School of Civil and Resources Engineering, The University of Western Australia*

## ABSTRACT

This paper reports on the ability of compensation grouting to reduce tunnelling induced settlements and investigates potential means of modelling such grouting numerically. The monitored movements of the 'Walsh building' during boring of two tunnels in Perth CBD (forming part of the MetroRail City Project) are used to show that compensation grouting (in sand) can greatly reduce movements. The 2D finite element (FE) back analyses indicated that the grouting can be modelled effectively in FE analysis by imposing a volumetric strain to the mass of soil subjected to grouting. Improved understanding of how grouting may be modelled numerically can increase the efficiency and cost-effectiveness of grouting.

## 1 INTRODUCTION

The New Metrorail City Project was designed and constructed by Leighton Kumagai Joint Venture (LKJV) for the Public Transport Authority (PTA) of Western Australia. The project consisted mainly of two bored tunnels (outer diameter 6.9 m) of 1.4 km combined length, two underground stations and cut and cover tunnels and dive structures of about 1 km total length in the Central Business District (CBD) of Perth. The two bored tunnels went either very close to or directly underneath some of the buildings and these buildings were treated with compensation grouting to mitigate the effects of tunnelling induced settlements. Keller Ground Engineering was appointed by LKJV for the compensation grouting and the instrumentation installation and monitoring was carried out by Fugro Spatial Solutions.

Compensation grouting is a process of injecting cement-based grout to compact the zones of soil under consideration. This procedure is widely used around the world to reduce tunnelling induced settlements. Compensation grouting can either be of the compaction variety for granular material or involve hydraulic fracturing to allow pathways for grout in clays. However there are few examples of successful compensation grouting carried out in granular soil (Baker *et al.*, 1983; Cording *et al.* 1989). To be successful, grouting needs detailed monitoring of the surface movement in conjunction with careful grout injection control.

The papers of Harris *et al.* (1994), Pototschnik (1992), Baker *et al.* (1983), Cording *et al.* (1989), Sugiyama *et al.* (2000), Kummerer *et al.* (2007), amongst others, describe how compensation grouting (CG) has been successful in reducing tunnelling induced building settlement. However in all of these cases, the grout injection was dictated and controlled by contemporaneous monitoring of movement. Research has now moved on into trying to develop an improved understanding of compensation grouting using analytical and numerical modelling. Better understanding of grouting mechanisms can improve efficiency and reduce grout quantities and costs. Some advances have been made (e.g. Addenbrooke *et al.*, 2002; Wisser *et al.*, 2005) but progress on numerical modelling is hampered by the relatively complex and varied grouting procedures used in practice. The compensation grouting carried out under the Walsh building (which is the focus of this paper) is simulated here using Plaxis 2D version 9.0 to assess the potential of a simple method of modelling the effects of compensation grouting numerically and to add to the limited number of published numerical back-analyses.

## 2 BUILDING DETAILS AND GROUND CONDITIONS

An aerial view of the TBM path and of the 'Gold group' and 'Walsh' buildings just south of the new William Street Station is shown in Figure 1. These buildings had shallow foundations and were considered vulnerable to tunnelling damage due to the close proximity to the tunnels. Compensation grouting was therefore implemented as a damage mitigation measure. After studying the feasibility of different methods, Keller employed hydro-fracture (hydraulic fracture) compensation grouting to protect the buildings during tunnel boring. Only the ground beneath the northern quarter of the Walsh building was to be treated.

The Walsh building, which is the focus of this paper, is heritage listed and has five elevated storeys and a basement. This building is a steel framed structure encased in concrete, with secondary reinforced concrete beams. The floors are also reinforced concrete (according to the property condition report prepared by Airey, Ryan & Hill Consulting Engineers, 2004). The original construction date, floor plans and foundation details of the building are unavailable, although it is understood that the building is on shallow foundations. This building

is about 35 m wide and 53 m in length (parallel to the tunnel). The alignment of the tunnels near Walsh building is indicated in Figure 1 and the front view of the Walsh building is shown in Figure 2.

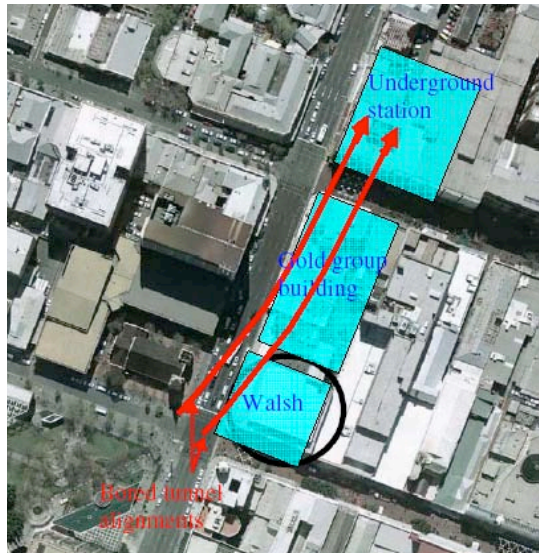


Figure 1: Aerial View of the Protected Buildings.

Figure 2: Front View of Walsh Building

The stratigraphy in Perth CBD comprises three formations. The bedrock or the 'Kings Park Formation' (KPF) underlies the over consolidated 'Perth Formation' (comprising interbedded layers of clay, silt and sand); normally consolidated 'Spearwood (aeolian) sand' overlies the 'Perth Formation' (alluvial). The stratigraphy at the Walsh building location (grouted area) shown in Figure 3 is based on nearby borehole and *in situ* test data (CPT & DMT). This shows that both Tunnel 1 and Tunnel 2 are within the alluvial silty and clayey layers of the Perth Formation at this location. The average CPT end resistance ( $q_c$ ) for each layer is also given in Figure 3;  $q_c$  data were not available below a reduced level of -10 m AHD. The (perched) water table in the Spearwood dune sand was observed to be at +8.6 m AHD and another water table was encountered at -2.3 m AHD in the Perth Formation (Golder Associates, 2003).

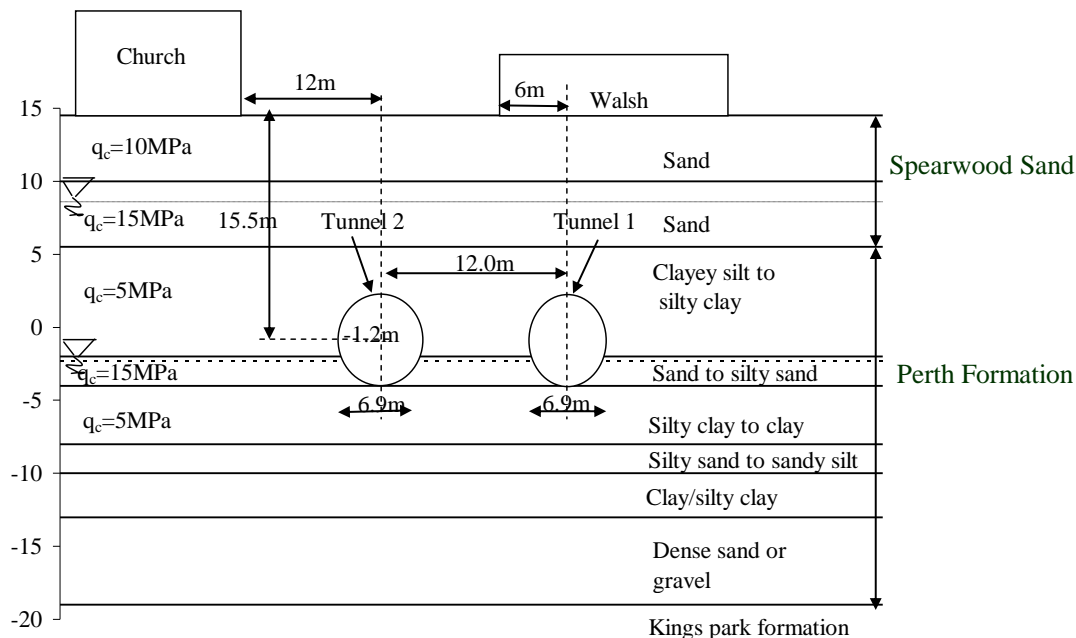


Figure 3: Soil Profile and Location of Tunnels near WALSH Building (Grouted area)

Figure 3 also indicates the relative position of the Walsh building and the tunnels at the north side of the building where the compensation grouting was carried out. The tunnel axis was about 17 m below ground level at the south side and 15.5 m deep on the north side. While Tunnel 1 gradually entered underneath the building at south side of the building, Tunnel 2 was away from the building throughout the length of the building (see Figure 1).

### 3 GROUTING

Hydro fracture compensation grouting involves two phases of grouting; the first phase, referred to as the condition phase grouting, is prior to any tunnelling to fill in the voids to improve the efficiency of subsequent active phase grouting. The details of the compensation grouting carried out for the Gold group buildings and the Walsh building are given by Williams and Nobes (2007). The grout was injected through arrays of TAM pipes (tubes-à-manchettes), all of which were located in the Spearwood dune sand at a distance of about 4m above the tunnel crown and 3.5 m below the building foundations. The TAM pipes were installed sub horizontally to a maximum length of 50 m from a temporary access shaft located on William Street. The schematic view of the Walsh building, approximate locations of tunnels, arrangements of grouting ports on TAM pipes and locations of Electro level (EL) beams on the building (to measure building tilt and hence vertical movement) are indicated in Figure 4. It is apparent from Figure 4 that only about a quarter of the plan area of the Walsh building was treated using compensation grouting.

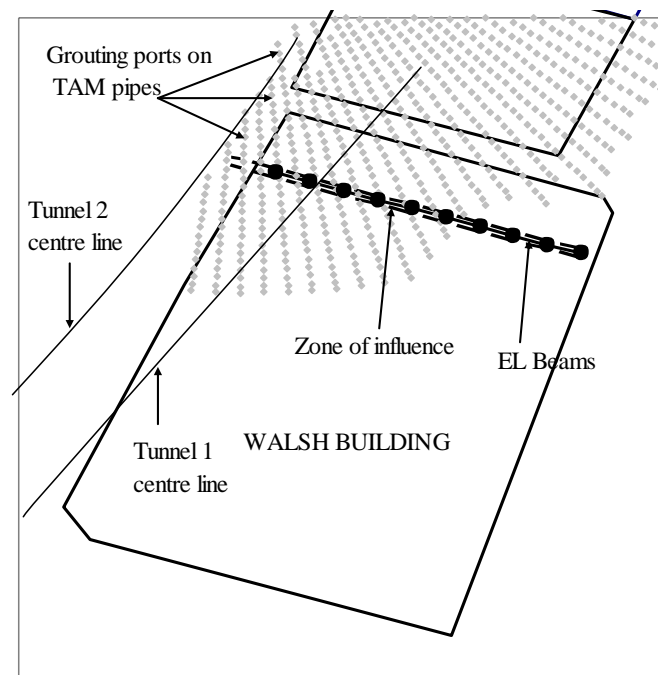


Figure 4: Arrangements of TAM Pipes under Walsh Building.

### 4 BUILDING MOVEMENT AFTER CONDITION PHASE GROUTING

For the conditioning phase, three passes of grouting were applied with a short rest period of about a day between passes. The real-time structural monitoring data summarised by Williams and Nobes (2007) indicated that there was little relaxation (i.e. settlement) after the rest period of the first and second passes of grouting (amounting to about 15% of the induced heave), while no settlement was observed after the 3<sup>rd</sup> pass (on completion of the grouting). By comparison, in soft Singapore marine clay, Addenbrooke *et al.* (2002) report a significant loss of heave (i.e. settlement) over a three day period immediately after the grouting finished due to the dissipation of excess pore pressure built up during grouting; such a phenomenon was not reported for (stiff) London clay.

The EL beams were located at about RL 21mAHD (6.5 m above the ground surface) on the northern façade of the Walsh building. The movements of the Walsh building, as inferred from the strings of EL beams and monitored anchor points after the grout conditioning phase (without considering the movements caused by TAM installation) are shown in Figure 5 and indicate a maximum heave of about 2.2 mm. The irregularity of the movement induced by the grout can be attributed to the non uniformity in the application of grout and this can be seen from Figure 6; this figure plots the volume of grout injected from TAM ports located within the zone of influence, which was assumed to be 0.5 m either side of the string of EL beams (see Figure 4). The volume of the heave profile is  $\sim 0.04 \text{ m}^3$  per metre width in the longitudinal direction and the total volume of the grout applied in the zone of influence was  $0.56 \text{ m}^3/\text{m}$ . These quantities indicate that the ratio of the grout volume injected to the heave volume was about 14. Further research is clearly needed to allow general assessment of the grout volume required to induce a required amount of heave.

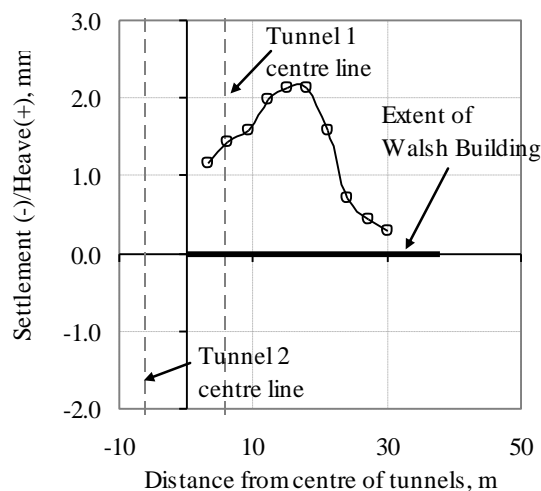


Figure 5: Movement of Building due to Condition Phase Grouting

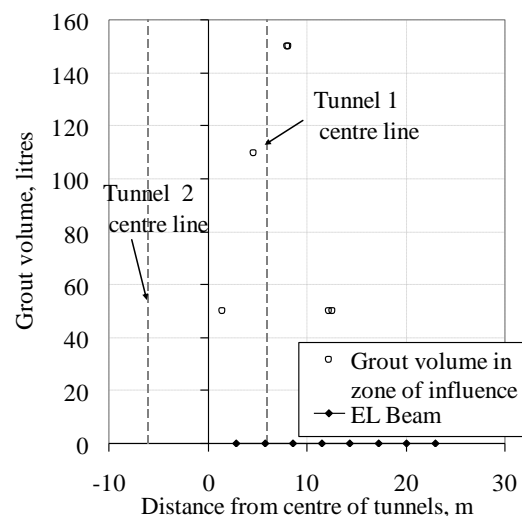


Figure 6: Variation of Grout Volume along the Transverse Direction of the Building

## 5 SURFACE AND BUILDING SETTLEMENT AFTER TUNNELLING

Since only a quarter (north side) of the Walsh building underwent compensation grouting, a comparison between the grouted area and non-grouted area provides an immediate indication of the effects of the grouting programme. The total volume of grout applied during boring of Tunnel 1 in the (assumed one metre wide) zone of influence from the TAM borehole was  $0.092 \text{ m}^3/\text{m}$ ; this is about one sixth of that applied during the condition phase grouting ( $0.56 \text{ m}^3/\text{m}$ ). The instrumentation at the Walsh building consisted of Surface Settlement Pins (SSP), Building Settlement Points (BSP) and EL beams (note that EL beams were only on the north side of the building). SSPs and BSPs are survey points either on the ground (SSP) or on the building (BSP).

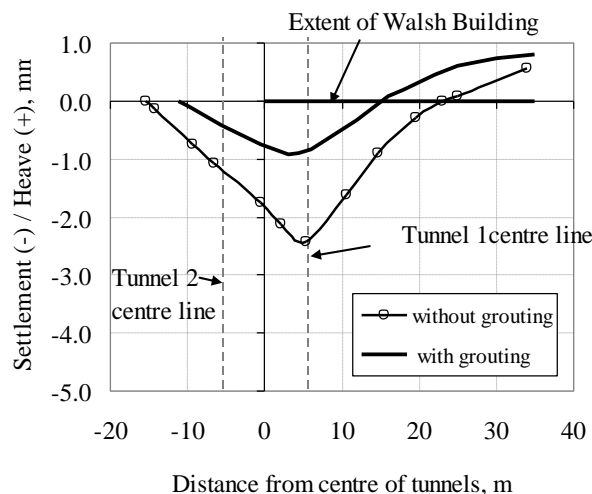


Figure 7: Surface Settlements due to Tunnel 1 Boring at Grouted and Non-Grouted Locations

Since no significant movement was observed during Tunnel 1 boring, active phase grouting (during tunnelling) was not carried out under Walsh building during Tunnel 2 boring. Hence only the transverse surface settlement troughs observed after completion of Tunnel 1 in the grouted and non-grouted areas are compared in Figure 7 and settlement trough measurements are summarised in Table 1. It is immediately apparent that grouting was successful in reducing settlements: maximum settlements were reduced by a factor of 2.5 and the ratio of the volume of the surface settlement trough to the nominal tunnel area (i.e. volume loss) was controlled to 0.03%. It is also worthy of note that in the non grouted area, the tunnel was not directly under the building as in the grouted area. The volume loss of 0.12% for Tunnel 1 in the non-grouted area is comparable with the observed

volume loss for Tunnel 2 adjacent to the non-grouted area of the Walsh building and at other building locations along the same route (Mathew, 2010). Heave on the eastern side of the Walsh building is observed for both cases – although it should be noted that, even in the ‘grouted area’, grout did not extend over the full width of the building. Another monitored building along the same route also showed heave at the far end of the building (Mathew, 2010).

Table 1: Summary of Settlement Troughs at Grouted and Non-Grouted Area of Walsh Building

	Non Grouted Area		Grouted Area	
	$S_{\max}$ (mm)	Volume Loss (%)	$S_{\max}$ (mm)	Volume Loss (%)
Tunnel 1	-2.42	0.12	-0.9	0.03

The building movement that took place during Tunnel 1 (note that no active phase grouting was carried out for Tunnel 2) is shown in Figure 8 and seen to be negligible. Although a comparison of building movements with and without grouting is not possible as there were no EL beams on the south side of the building (non –grouted area), the settlement pattern of the ground and building movement obtained from the SSPs and BSPs (Figure 7 ) indicates that the grouting significantly reduced the building settlement as well.

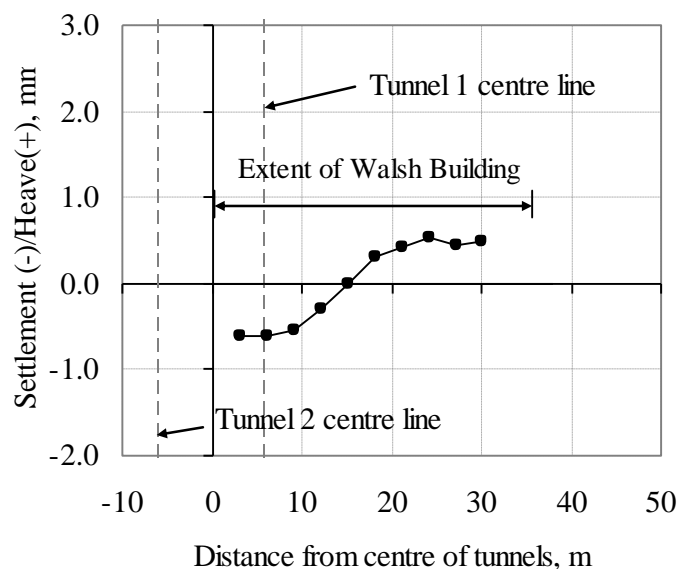


Figure 8: Building Movement due to Grouting and Tunnel 1 Boring.

## 6 NUMERICAL MODELLING

As mentioned earlier, relatively few published studies report on the numerical modelling of compensation grouting. Although the actual specific details and procedures of compensation grouting cannot be modelled in detail, an attempt is made here to investigate if the application of a volumetric strain in the grouted zone in a Plaxis 2D analysis could capture the essential features of the grouting process and its influence on soil-structure interaction.

### 6.1 SOIL MODEL

The Hardening Soil model with small strain stiffness (HSSmall) was used for the 2D finite element analysis. The HSSmall model is an extension of the original Hardening Soil model (HS model), developed by Schanz *et al.* (1999) and implemented in Plaxis. The HS model is a non-linear elastic plastic formulation which adopts multiple yield loci as a function of plastic shear strain and a cap to allow volumetric hardening. Loading and unloading within the current yield surface are assumed elastic (defined by a separate modulus,  $E_{ur}$ ) and the Mohr Coulomb failure criterion is employed. The extension uses a “Small Strain Overlay” (Benz, 2006) to detect small strain amplitudes and applies comparatively higher stiffness values for computations at these small strain levels. The overlay is inactive for large strain amplitudes, when the soil response is determined by the HS model. Changes in loading direction may re-activate the overlay.

## 6.2 SOIL PARAMETERS

The HSSmall soil parameters selected for the Spearwood sand (SS) and Perth Formation (PF) sand and clay at a reference stress ( $P_{ref}$ ) of 100 kPa are shown in Table 2; note that the normalised parameters for the sandy beds of the Perth Formation are assumed similar to the Spearwood Sand.  $E_{50}^{ref}$  is the secant stiffness in a standard drained triaxial test at the reference stress,  $G_0^{ref}$  is the small strain shear modulus at the reference stress and  $\gamma_{0.7}$  is the shear strain level at which the secant shear modulus  $G$  is reduced to 70% of  $G_0$ . These soil parameters were derived from the field tests as well as the laboratory tests carried out on the undisturbed soil samples collected from the site. A detailed description of the laboratory study on the undisturbed soil samples and estimation of soil parameters are given in Mathew (2010).

Table 2: HSSmall Soil Model Parameters

Description of soil	Type	$E_{50}^{ref}$ (MPa)	$\phi'$ ( $^\circ$ )	$\nu_{ur}$	$G_0^{ref}$ (MPa)	$\gamma_{0.7}$ (%)
Sand and silty sand	Drained	114	35	0.15	220	0.005
Clay, clayey silt and silty clay	Undrained	68	28	0.15	130	0.002

## 6.3 MODELLING OF BUILDING, TUNNEL AND GROUTING

Since the exact building details of the Walsh Building were unavailable, input parameters for the building were selected based on assumed dimensions (derived through discussions with structural engineers); beams were taken to be 350 mm  $\times$  650 mm deep, columns as 500 mm square and the foundation was assumed to be a 1.35 m thick raft. Plate elements were used to model the building components and the input parameters such as axial stiffness ( $EA$ ) and bending stiffness ( $EI$ ) are summarised in Table 3. The modulus of elasticity ( $E$ ) of the concrete was assumed to be 20 GPa. The tunnel lining was modelled using elastic shell elements with a Young's modulus of 35 GPa, Poisson's ratio of 0.15 and thickness of 0.275 m. A dead load (DL) of 5 kPa and live load (LL) of 3 kPa were assumed for load take down calculations.

Table 3: Input Parameters for the Building Components

	$EI$ (MNm <sup>2</sup> /m)	$EA$ (MN/m)
Beam	168	4777
Column	109	5250
Raft	4310	28350

The mesh showing the building, tunnels and the location of compensation grouting (CG) are shown in Figure 9. The width of the model adopted was 100 m to minimise boundary effects. Both vertical boundaries were restrained against horizontal movement and rotation. The bottom boundary was restrained against vertical and horizontal movement. A no flow and a no consolidation boundary were specified at the base to represent impermeable rock.

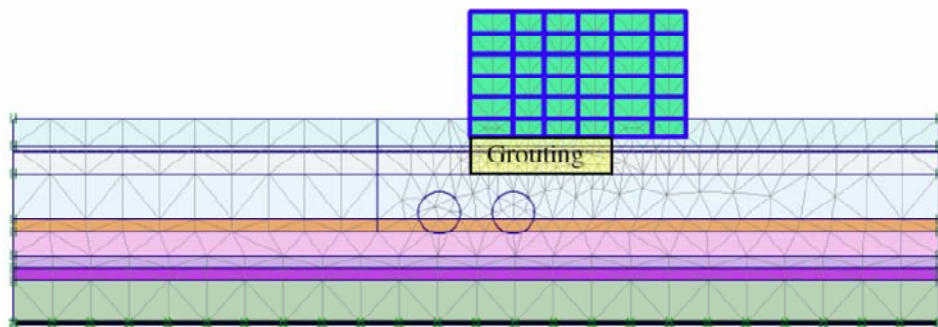


Figure 9: Mesh Showing the Tunnels, Building and Location of the Grouting



The TAM pipes were located approximately midway between the tunnel crown and the building foundations (Williams and Nobes, 2007). Although the area occupied by the grout is not known, it was assumed that grouting was effective in the sand present from the foundation level (at +11.0 mAHD) down to the silty clay layer (with top level at +5.5 mAHD). Compensation grouting was modelled by applying a volumetric strain to the complete 5.5m thickness of this sand in the area indicated in Figure 9. A second analysis involved application of a volumetric strain to a zone 1m thick (rather than 5.5 m) at the elevation of the TAMs, and it was found that the overall additional volume that needed to be applied to induce observed levels of building heave was approximately the same in both sets of analysis.

#### 6.4 PREDICTED VERSUS MEASURED BUILDING MOVEMENT AFTER CONDITION PHASE GROUTING AND ACTIVE GROUTING

As mentioned earlier, the condition phase grouting was carried out prior to tunnelling to tighten the soil. Prior to grouting, the building was activated in Plaxis and the ground consolidated to a minimum excess pore pressure of 1k Pa to initiate the *in situ* conditions. The condition phase grouting was then modelled by imposing a volumetric strain in the grouted area as indicated in Figure 9 and consolidated again to dissipate any excess pore pressure developed. To simulate the cementation caused by grouting, a nominal 'smeared' *c*' (cementation) value of 10 kPa was specified to the sand in the grouted area. It was found that application of an increase in volume  $0.1 \text{ m}^3/\text{m}$  to the grouted area (which equates to a volumetric expansion of 0.09% in the grouted zone shown on Figure 9) provided the best match between observed and predicted heave, as shown on Figure 10; the heave volume for both cases is  $0.04 \text{ m}^3/\text{m}$ . The increased volume of the grouted area equates to about one fifth of the estimated grout volume injected ( $0.56 \text{ m}^3/\text{m}$ ) and is about three times the heave volume. The difference in shape between the predicted and measured heave profiles on Figure 10 may reflect non-uniformities in the grouting volumes as seen on Figure 6.

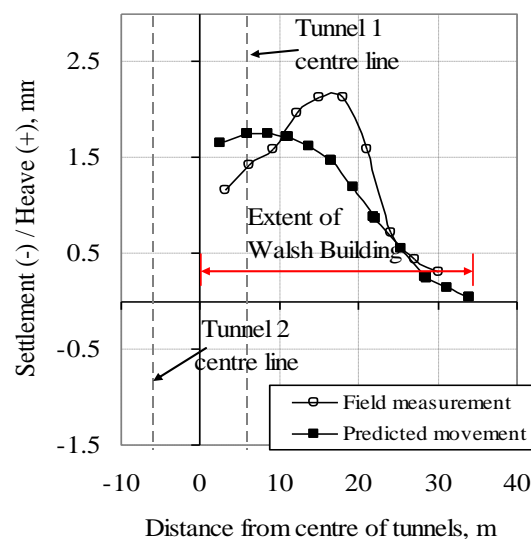


Figure 10: Observed and Predicted Movement after Condition Phase Grouting.

After the dissipation of the excess pore pressures due to condition phase grouting, the first tunnel was excavated and a lining was installed. A volumetric strain of 0.03% was applied in the next step to the improved sand to represent the active phase grouting along with a contraction of the tunnel of 0.03% (applied at the centre point of the tunnel; see Table 1 for measured volume loss at grouted area), which was the volume loss due to tunnelling in the grouted area. The excess pore pressure generated from the tunnelling and the grouting was then dissipated in the next consolidation step.

The comparison of the predicted and the measured vertical movement of the building after Tunnel 1 boring are shown in Figure 11. The volumetric strain (0.03%) to model the active phase grouting is one third of that applied during the condition phase grouting (0.09%). However the actual volume of grout injected ( $0.09 \text{ m}^3$ ) was about one sixth of that applied during the conditioning phase, indicating that the efficiency of grouting in the active phase improved due to the prior condition phase grouting. Although the grouting was modelled effectively by the finite element method, more laboratory and field investigation is required to allow designers to assess the relationship between the degree of volumetric strain to be imposed and the grout volume injected in different soil conditions.

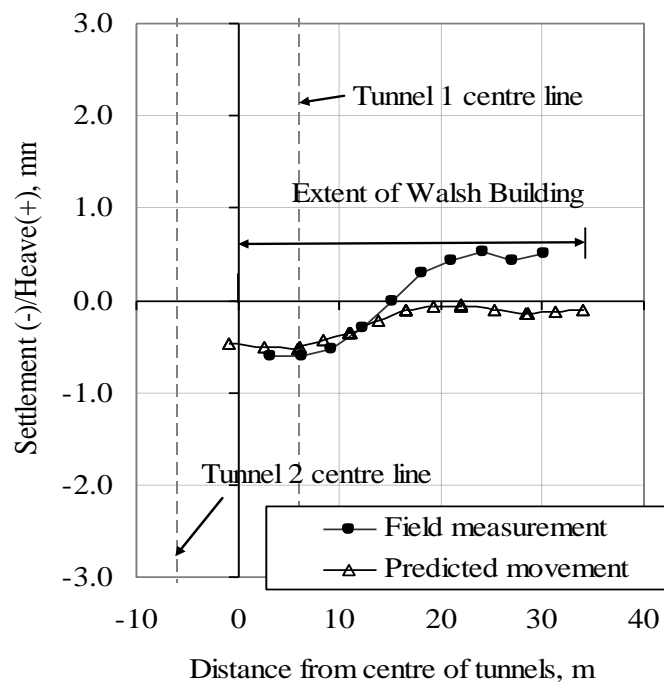


Figure 11: Observed and Predicted Movement of Building due to Tunnel 1

## 7 CONCLUSIONS

The effect of compensation grouting (hydraulic fracture) in Spearwood sand was assessed from the monitored movement of the Walsh building, the northern portion of which had undergone grouting. The tunnels were located primarily in silty and clayey layers of the Perth Formation. Numerical back analyses using Plaxis 2D have been carried out to investigate a simple means of modelling grouting numerically. Some conclusions from this study are as follows:

- Compensation grouting in the Spearwood sand was successful in reducing building movements to one quarter of those experienced if no treatment was undertaken.
- Large grout volumes were required during the grout conditioning phase due to the relatively high porosity of the Spearwood dune sand.
- The effect of grouting on buildings can be modelled effectively in FE analysis by imposing a volumetric strain to the mass of soil subjected to grouting. However further research is needed to allow designers to assess the relationship between the degree of volumetric strain imposed and the grout volume injected.

## 8 ACKNOWLEDGEMENTS

The grout data and other relevant information provided by Keller Ground Engineering via Leighton Kumagai Joint Venture (LKJV) is gratefully acknowledged. The authors also acknowledge the funding provided by an Australian Research Council (ARC) linkage grant in association with LKJV. LKJV are also thanked for providing the field soil test data and instrumentation data for this research.

## 9 REFERENCES

- Addenbrooke, T.I., Ong, J.C.W. and Potts, D.M. (2002). Finite-element analysis of a compensation grouting field trial in soft clay. *Proc. Institution of Civil Engineers, Geotechnical Engineering*, Vol. 155, issue 1, 47-58.
- Airey, Ryan & Hill (2004). Property condition report- Building No.24 – Walsh building.
- Baker, W.H., Cording, E.J. and MacPherson, H.H. (1983). Compaction grouting to control ground movements during tunnelling. *Underground Space*, Vol.7, 205-212.



- Benz, T., (2006). *Small-Strain Stiffness of Soils and its Numerical Consequences*. Ph.D. Thesis, Stuttgart Universität.
- Cording, E.J., Brierley, G.S., Mahar, J.W. and Boscardin, M.D. (1989). Controlling ground movements during tunnelling. *Art and Science of Geotechnical engineering at the Dawn of the 21<sup>st</sup> Century*, Pentice-Hall, New Jersey, USA, 477-505.
- Golder Associates (2003). *Geotechnical and Hydrogeological investigation report*.
- Kummerer, C., Thurner, R., Rigazio, A., and Zamagni, A. (2007). *Proc. 14th European Conference on Soil Mechanics and Geotechnical Engineering*, Madrid, Vol.3, 1269-1274.
- Harris, D.I., Mair, R.J., Love, J.P. Taylor, R.N. and Henderson, T.O. (1994). Observations of ground and structure movements for compensation grouting during tunnel construction at Waterloo Station, *Geotechnique*, Vol. 44, No.4, 691-713.
- Mathew, G.V. (2010). *Analysis and interpretation of ground and building movements due to EPB tunnelling*. PhD Thesis, University of Western Australia
- Pototschnik, M.J. (1992). Settlement reduction by soil fracture grouting. *ASCE Speciality conference on Grouting, Soil Improvement and Geosynthetics*, New Orleans, 398-409.
- Schanz, T., Vermeer, P.A. and Bonnier, P.G. (1999). Formulation and verification of the Hardening-Soil Model. *Beyond 2000 in Computational Geotechnics*, Balkema, R.B.J. Brinkgreve, Rotterdam, 281-290.
- Sugiyama, T., Nomoto, T., Ano, Y. and Hagiwara, T. (2000). Compensation grouting at the Docklands Light Railway Lewisham Extension project. *Geotechnical Aspects of Underground Construction in Soft Ground*, Kusakabe, Fugita & Miyazaki (eds), Balkema, Rotterdam, 319-324.
- Williams, M. and Nobes, C. (2007). Soilfrac compensation grouting for building protection on the new MetroRail City Project. . *Proc. Seminar on New MetroRail City Project, Tunnelling and Structures*, Perth, 27-42.
- Wisser, C., Augarde, C.E., and Burd, H.J. (2005). Numerical modelling of compensation grouting above shallow tunnels. *International journal for numerical and analytical methods in geomechanics*, 29, 443-471.

